Published in final edited form as:
Chem Sci. 2014 April 1; 5(4): 1642–1649. doi:10.1039/C3SC53301H.

Inhibition of the 4Fe-4S Proteins IspG and IspH: an EPR, ENDOR and HYSCORE Investigation

Francisco Guerra[a,‡], **Ke Wang**[b,‡], **Jikun Li**[a], **Weixue Wang**[a,§], **Yi-Liang Liu**[a], **Shivani Amin**[c], and **Eric Oldfield**[a,b]

Eric Oldfield: eoldfiel@illinois.edu

[a]Center for Biophysics and Computational Biology, University of Illinois at Urbana-Champaign, 607 South Mathews Avenue, Urbana, IL 61801

[b]Department of Chemistry, University of Illinois at Urbana-Champaign, 600 South Mathews Avenue, Urbana, IL 61801

[c]Department of Chemical and Biomolecular Engineering, University of Illinois at Urbana-Champaign, 600 South Mathews Avenue, Urbana, IL 61801

Abstract

IspG and IspH are proteins that are involved in isoprenoid biosynthesis in most bacteria as well as in malaria parasites and are important drug targets. They contain cubane-type 4Fe-4S clusters that are involved in unusual $2H^+/2e^-$ reductions. Here, we report the results of electron paramagnetic resonance spectroscopic investigations of the binding of amino- and thiolo-HMBPP (HMBPP=*E*-1-hydroxy-2-methyl-but-2-enyl 4-diphosphate) IspH substrate-analog inhibitors to both proteins, as well as the binding of HMBPP and an acetylene diphosphate inhibitor, to IspG. The results show that amino-HMBPP binds to reduced IspH by Fe-C π-bonding with the olefinic carbons interacting with the unique 4th Fe in the 4Fe-4S cluster, quite different to the direct Fe-N ligation seen with the oxidized protein. No such π-complex is observed when amino-HMBPP binds to reduced IspG. No EPR signal is observed with IspH in the presence of dithionite and thiolo-HMBPP, suggesting that the 4Fe-4S cluster is not reduced, consistent with the presence of a 420 nm feature in the absorption spectrum (characteristic of an oxidized cluster). However, with IspG, the EPR spectrum in the presence of dithionite and thiolo-HMBPP is very similar to that seen with HMBPP. The binding of HMBPP to IspG was studied using hyperfine sublevel correlation spectroscopy with ^{17}O and ^{13}C labeled samples: the results rule out direct Fe-O bonding and indicate π-bonding. Finally, the binding to IspG of a potent acetylene diphosphate inhibitor was studied by using electron-nuclear double resonance spectroscopy with ^{13}C labeled ligands: the large hyperfine couplings indicate strong Fe-C π-bonding with the acetylenic group.

Correspondence to: Eric Oldfield, eoldfiel@illinois.edu.

[§]Present address: Department of Chemistry, Massachusetts Institute of Technology, 77 Massachusetts Ave. Cambridge, MA 02139

[‡]These authors contributed equally to this work.

[†]Electronic Supplementary Information (ESI) available: [Details of compound syntheses, protein expression and purification, inhibition assays, EPR, HYSCORE, and ENDOR sample preparation and spectral simulations. EPR *g*-values in Table S1. Protein inhibition assay data Table S2 and Figure S4. Additional HYSCORE spectra and simulations in Figures S1–S2, S5–S9 and S11. EPR and UV-Vis spectra of IspH and inhibitor **8** in Figure S3. Additional CW EPR spectra of IspG in Figures S10, S12 and S13.]. See DOI: 10.1039/b000000x/

These results illustrate a remarkable diversity in binding behavior for HMBPP-analog inhibitors, opening up new routes to inhibitor design of interest in the context of anti-bacterial and anti-malarial drug discovery, as well as “cubane-type” metallo-biochemistry, in general.

Introduction

There is currently great interest in the structure, function and inhibition of the enzymes involved in the 2-*C*-methylerythritol 4-phosphate (MEP) or ‘non-mevalonate’ isoprenoid biosynthesis pathway.[1] This pathway is present in most bacteria as well as in the protozoan parasite, *Plasmodium falciparum*, the causative agent of the most common and serious form of malaria.[2,3] This pathway is not used by humans and is essential for survival and is, therefore, an important drug target. In addition, the MEP pathway is present in plants, making inhibitors of interest as potential herbicides. The last two steps in the pathway are $2H^+/2e^-$ reductions carried out by 4Fe-4S cluster-containing proteins (Scheme 1) in which there are unique 4th iron atoms in the cluster that are not coordinated to protein Cys residues. The penultimate protein in the pathway is IspG, 2-*C*-methyl-D-erythritol-2,4-*cyclo*-diphosphate (**1**) reductase (also known as GcpE), which catalyzes the reduction of 1 to *E*-1-hydroxy-2-methyl-but-2-enyl 4-diphosphate (HMBPP; **2**). The last enzyme in the pathway is IspH, HMBPP reductase (also known as LytB) and catalyzes the reduction of HMBPP to isopentenyl diphosphate (IPP, **3**) and dimethylallyl diphosphate (DMAPP, **4**), in a ~ 5:1 ratio. The structures of both the bacterial IspG and IspH proteins are known.[4–7] IspG contains two domains: a TIM barrel (A) involved in binding the diphosphate group of **1** as well as in providing H^+, and a 4Fe-4S cluster containing domain (B), involved in reduction, and in recent work the structure of **1** bound to a bacterial IspG has been reported.[8] The bacterial proteins function as “head-to-tail” dimers with the TIM (triose phosphate isomerase) barrel of one partner in the dimer associated with the 4Fe-4S cluster-containing domain of the other molecule in the dimer.[6–8] In plant and malaria parasite IspGs, there is also a third domain (A*), located between the A and B domains. The A* domain has essentially no sequence conservation between different organisms, but has been proposed to again adopt a TIM (triosephosphate isomerase) barrel fold and act in a primarily structural capacity, enabling the A and B domains in a monomer to come together and function catalytically.[9] IspH is also modular and contains three αβ domains, the 4Fe-4S cluster being buried at the center of the trimeric structure.[4,5]

In previous work we reported that two classes of molecules, acetylenes and pyridines,[10–13] acted as modest IspH inhibitors, binding at or close to the 4th Fe of the 4Fe-4S cluster, with the acetylenes also inhibiting IspG[9,11] with IC_{50} values as low as 0.77 μM. More recently, the amine analog of **2**, **7** as well as the thiol analog **8** have been reported[14] to be even more potent IspH inhibitors (IC_{50} ~ 0.2 μM) and it was shown via Mössbauer spectroscopy and quantum chemical calculations that both bound to the oxidized ($[Fe_4S_4]^{2+}$) form of IspH, forming Fe-N and Fe-S bonds, respectively, with the 4th Fe. Here, we report that IspG is likewise inhibited by these compounds. We also present the results of EPR[15] and HYSCORE (hyperfine sublevel correlation spectroscopy[16,17]) investigations into the nature of the inhibition of both IspH as well as IspG by **7** and **8**, in the presence of sodium dithionite; and ENDOR (electron nuclear double resonance[16,18]) spectroscopic examination

of the inhibition of IspG by **5** using two selectively ^{13}C-labeled species, and of the binding of **2** to IspG, using uniformly as well as three specifically ^{13}C-labeled ligands.

Results and discussion

Binding of amine and thiol inhibitors to IspH

We first investigated the question of how **7** and **8** might bind to the reduced form of IspH, since they are known to bind via N or S to the oxidized ($[Fe_4S_4]^{2+}$) protein. Is this also the case with reduced IspH? To do this, we used EPR and HYSCORE spectroscopy. We began by investigating binding of the amine ligand **7** to *Aquifex aeolicus* IspH (*Aa*IspH), *Plasmodium falciparum* IspH (*Pf*IspH), and *E. coli* IspH (*Ec*IspH). The 9.05 GHz EPR spectrum (at 10K) of dithionite-reduced *Aa*IspH was reported previously[19] to be a mixture of an $S = {}^1/_2$ and $S = {}^3/_2$ species, with the $S = {}^1/_2$ species having *g*-values of 2.040, 1.919, 1.849 (Table S1).

The $g \sim 2$ region in the absence of any added ligand is shown for reference in Figure 1A. The spectrum is similar to that found with other 4Fe-4S proteins, such as aconitase.[20] On addition of **7**, a sharp new feature appears (having g_i = 2.134, 2.006, 1.973, Table S1). With *Pf*IspH and *Ec*IspH, there is only very weak signal intensity in the absence of added ligands, but in both cases in the presence of **7** intense and sharp signals with $g_i \sim$ 2.137, 2.007, 1.980, Table S1, are seen (Figure 1C,D) suggesting that the ligand binds at or close to the $[Fe_4S_4]^+$ cluster in all three IspHs. The question then arises as to how **7** binds. There are two main possibilities: First, **7** binds via its NH_2 group to the $[Fe_4S_4]^+$ cluster in basically the same manner as that proposed for binding to the oxidized cluster, i.e. by forming a Fe-N bond to the 4th Fe.[14] Second, **7** might bind to IspH with its aminomethyl group “rotated-out”, away from the cluster, interacting with E126, as proposed earlier[11] for the CH_2OH group in the HMBPP substrate, as now seen crystallographically[21] with HMBPP, and as confirmed by ^{17}O-HYSCORE spectroscopy.[22]

To help distinguish between these two possibilities, we obtained the HYSCORE spectra of **7** bound to *Aa*IspH, Figure 2A, as well as to *Pf*IspH and *Ec*IspH, Figures S1 and S2. To distinguish any ^{14}N hyperfine interaction with the protein backbone from that with the ligand **7**, we also obtained the HYSCORE spectrum of **7** bound to ^{15}N-labeled *Aa*IspH, Figure 2B. If there were a Fe-N bond present in the complex, we would expect a sizeable ^{14}N hyperfine coupling since there would be a strong metal-ligand orbital overlap facilitating spin density transfer from the metal to the ligand. For example, with the pyridine inhibitor **9** bound to IspH,[13] as shown in Figure 2C, the ^{14}N hyperfine interaction A_{iso} (^{14}N) is ~ 8 MHz and we previously noted that, on average, A_{iso} (^{14}N) values were ~ 6 MHz for a series of proteins containing Fe-N bonds. Given that there is no large hyperfine coupling observed (Figure 2A, B), we conclude that there is no direct Fe-N bond in the reduced IspH + **7** complex. In addition, the g_i, g_{iso} and Δg values for IspH + **7** are essentially identical to those we find with HMBPP (**2**) bound to both *E. coli* and *A. aeolicus* IspH mutants (Table S1, shown graphically in Figure 3), supporting similar binding of both **2** and **7**. Plus, the spectrum of the pyridine inhibitor **9** bound to IspH is very broad, quite different to the sharp spectrum found with **7**. We thus propose that **7** binds to IspH in basically the same manner

as does HMBPP (**2**), and a model based on the "rotated-out" HMBPP X-ray structure[21] in which the HMBPP ligand's OH group is replaced by an NH_3^+ group is shown in Figure 2D. As can be seen in this (HMBPP X-ray based) structural model, the ligand's $CH_2NH_3^+$ group can interact with the E126 carboxylate, providing strong Coulombic interactions that may help account for its potent IspH inhibition (where assays are carried out under reducing conditions).

As we reported previously[22], there are three major clusters in this (Figure 3) and related $\Delta g/g_{iso}$ plots[22]: classic $[4Fe–4S]^+$ clusters where $g_{iso} < g_e$, from proteins such as ferredoxins, aconitase, and ligand-free IspH/IspG; oxidized HiPIPs and synthetic $[4Fe–4S]^{3+}$ models with $g_{iso} > g_e$ and $[4Fe–4S]^+$ clusters with alkene or alkyne ligands where $g_{iso} > g_e$ but where the g_{iso}-values are generally smaller than those of typical HiPIPs. Clearly, the amine inhibitor **7** falls in the "ligand free" region discussed earlier, that is, the nitrogen does not bind directly to Fe.

Interestingly, there is a small feature centered close to (−1.5, 1.5) MHz in all three *Aa*IspH +**7,** *Pf*IspH+**7** and *Ec*IspH+**7** spectra that has not been seen previously with any other ligands. It did not change when ^{15}N-labeled *Aa*IspH protein was used instead of natural abundance *Aa*IspH (Figure 2B), so it does not arise from a ^{14}N hyperfine coupling with the protein backbone. The feature can be simulated with a ^{14}N hyperfine interaction having $\boldsymbol{A}_i$ = [1.85, 1.25, 3.70] MHz, A_{iso} = 2.33 MHz, e^2qQ/h = 0.8 MHz, η = 0.2 (Figure S2). The quadrupole coupling constant is consistent with that expected for an alkyl ammonium[23] group ($e^2qQ/h \sim 0 – 1$ MHz) and the hyperfine coupling anisotropy suggests close proximity to the paramagnetic center, consistent again with the "rotated-out" model proposed above.

We next investigated binding of the thiol ligand **8**, to *Ec*IspH. The IC_{50} values for **7** and **8** in inhibiting *Ec*IspH are very similar and both bind to the oxidized protein, forming Fe-N and Fe-S bonds, respectively, with the 4th Fe in the cluster.[14] However, the electronic structure of the complex with **8** is spin-delocalized while that with **7** is spin-localized, suggesting that there might be significant differences in electronic structure between **7** and **8** when bound to reduced IspH.

The EPR spectrum of *Aa*IspH in the presence of sodium dithionite is shown in Figure S3A (in blue) and is characteristically broad, as is the case without the substrate. However, essentially no signal is seen in the $g \sim 2$ region (or at lower field, Figure S3A inset) for a sample incubated with dithionite in the presence of the thiol ligand **8** (Figure S3A, in red), unlike the situation with **7**. This suggested to us the possibility that in the presence of the thiol ligand, the cluster might not be reduced, that is, it remains in the oxidized, $S = 0$ state. This appears to be the case, as illustrated in the UV-VIS spectra shown in Figure S3B. The spectrum of oxidized ($[Fe_4S_4]^{2+}$) IspH (blue trace) shows a characteristic peak at ~ 420 nm, which disappears on dithionite reduction (green trace). The spectrum of oxidized IspH + **8** (red trace) is similar to that of the oxidized protein in the absence of **8**; however, addition of dithionite minimally changes the spectrum; the shoulder at ~ 420 nm is still seen with IspH + **8** + dithionite. We also find that addition of **8** to dithionite-reduced IspH generates the 420 nm shoulder (superimposed on the large dithionite background peak), suggesting that

reduced IspH+**8** is relatively unstable, consistent with the lack of any EPR signal for this system, Figure S3A.

Binding of amino, thiol inhibitors and HMBPP to IspG

We next investigated the inhibition of IspG (GcpE) by **7** and **8**. As can be seen in Supporting Information Figure S4, **7** and **8** both inhibit IspG. The IC_{50} values are in the range 0.8–2.5 μM (Supporting Information Table S2). The EPR spectra of the thiol **8** bound to the (two-domain) bacterial IspGs (from *E. coli* and *P. aeruginosa*) are shown, together with their spectral simulations and data for the three domain *Arabidopsis thaliana* IspG, in Figure 4A–C. All three spectra have very similar g_i (Table S1) and hence, g_{iso} (~ 2.03) and Δg (~ 0.13) values (Figure 3), indicating little inter-species variability, as well as no differences between the 2- and 3-domain proteins. Very similar results are found with **2** (HMBPP, containing an OH group) bound to the same proteins, Figure 4D–F, although on average the g_{iso} and Δg values found with **2** are slightly smaller, Table S1. It might be assumed that both **2** and **8** would bind to the unique 4th iron in the same way, via Fe-O or Fe-S bonds. However, it is also possible that there are no direct Fe-O or Fe-S bonds arising from these ligands, in reduced IspG. Of course, strong EPR signals are seen with e.g. 4Fe-4S ferredoxins, but there, g-values are rather different, on average $g_3 = 1.91$, $g_{iso} = 1.97$ and Δg ($= g_1 - g_3$) ~ 0.15,[22,24] to be compared with the average values of g_3 ~ 1.98, $g_{iso} = 2.03$ and Δg ~ 0.12 for **2** and **8** bound to the IspGs, Table S1.

To investigate HMBPP binding in more detail, we synthesized the [1-^{17}O] analog of **2**, labeled at the terminal (1-CH_2OH) group, and obtained a HYSCORE spectrum, Figure 5A. (For more spectra acquired at different field positions and τ values, see Figure S5) There is no evidence for any ^{17}O HYSCORE signal, suggesting that there is no direct Fe-O bond to the ligand, **2**. For purposes of comparison, the HYSCORE spectrum of the ^{17}O-labeled IspG reactive intermediate "X", shown in Figure 5B, exhibits an intense signal (data from Wang et al.[10]), proposed earlier to arise from a ferraoxetane species (i.e. a species containing an Fe-O bond). We thus propose that since we see no evidence for any ^{17}O hyperfine coupling that **2** (HMBPP) binds to the 4Fe-4S cluster by another mechanism, e.g. π-bonding. This would be similar to the mechanism proposed earlier for the isomer of HMBPP (**10**) binding to the *Ec*IspH E126Q mutant[22] in which the g-values are essentially identical (with g_1 ~ 2.09; g_{iso} ~ 2.03, Δg ~ 0.10) to those seen with **2** bound to *Ec*IspG (g_1 ~2.09, $g_{iso} = 2.03$, Δg ~ 0.12, Table S1). The strong similarity in the EPR spectra of **2** and **8** bound to IspG would then suggest that the thiol ligand binds in a similar manner, consistent with the observation that these spectra are quite unlike those of reduced ferredoxins.[24] To investigate the interaction between HMBPP carbon atoms and the IspG [4Fe-4S] cluster, we obtained HYSCORE spectra of [*U*-^{13}C], [1-^{13}C], [2-^{13}C], and [3-^{13}C] HMBPPs bound to reduced IspG, Figure 6. There were no large hyperfine couplings observed with the [*U*-^{13}C] labeled ligand, Figure 6A, unlike the ~17 MHz hyperfine coupling seen for **1** bound to IspG.[25] ENREF 24 To assign the resonances that were observed we next investigated the three selectively ^{13}C-labeled HMBPPs: spectra are shown in Figure 6B–D. The results of spectral simulations (Figures S5–S9) using EasySpin[26,27] yielded the hyperfine coupling tensors shown in SI Table S3: [1-^{13}C], $\boldsymbol{A_{ii}}$ = [−0.7, −0.9, 2.2] MHz; [2-^{13}C], $\boldsymbol{A_{ii}}$ = [0.5, 0.7, 4.9] MHz; [3-^{13}C], $\boldsymbol{A_{ii}}$ = [3.9, −0.3, −0.1] MHz. Clearly, all three hyperfine interactions are

quite small, although those for the 2 and 3-positions (the double bond) are larger than for C-1, consistent again with a weak π-interaction.

In sharp contrast to the results with **2** and **8**, with the amine ligand **7** binding to *Ec*IspG we find a very broad spectrum (Figure S10A) that has similar g_i, g_{iso} and Δg values to those found with the "un-liganded" protein (Figure S10B, Table S1) - in which of course OH, H_2O or a protein ligand might be bound to the 4th Fe. We see no evidence for a Fe-N interaction in the HYSCORE spectrum, Figure 5C (also at 3 other fields, Figure S11), plus, we find that the amine ligand **7** displaces HMBPP (**2**) from *Pa*IspG on a tens-of-seconds timescale, as shown in Figure S10C,D. Here, the HMBPP signals (red arrows, Figure S10C) arise from adventitiously bound HMBPP that co-purified with the *Pa*IspG protein.

What is surprising about the results with IspG is how different they are to those found with IspH, given that both proteins have similar 4Fe-4S clusters with unique 4th Fe atoms, and both carry out $2H^+/2e^-$ reductions. Specifically, with IspH, the amine ligand **7** binds to the reduced protein; the resulting EPR spectrum is very similar to that found with the IspH substrate HMBPP (**2**) bound to an E126Q mutant; and there is no large ^{14}N HYSCORE signal – all suggesting π-bonding of a "rotated-out" $–CH_2NH_3^+$ species, while with the thiol inhibitor **8**, the IspH 4Fe-4S cluster is not reduced, so inhibition is due to binding to oxidized protein. With IspG, the cluster can be reduced in the presence of **2**, **7**, or **8**. The EPR spectra of **2** (HMBPP) and **8** (the thiol ligand) bound to IspG are very similar to each other, but there is no ^{17}O hyperfine coupling (or it is very small), suggesting no direct Fe-O bonding (or Fe-S bonding, with **8**). Plus, there are only weak interactions between the π-bond in **2** and the cluster, based on the ^{13}C HYSCORE results. With the amine-ligand **7**, the EPR spectrum is similar to that seen with ligand-free protein (and the Δg, g_{iso} values cluster in the "ligand-free region" in Figure 3), and there is no evidence for Fe-N bonding, in which case it seems likely that water or protein ligands (or both) bind to the 4th Fe. These results are also supported by the observation that spectra of **2** + *Pa*IspG can be seen at both 10 and 20 K, Figure S12A, but only at 8 K with **7**, Figure S12B. That is, the HMBPP-bound spectrum, as with other HiPIP-like spectra, is sharp and does not broaden at higher temperatures, while the spectrum of **7** bound to IspG is broad and has almost disappeared at 20K, as seen in conventional σ-complexes.

Based on computational docking (with AutoDock Vina[28]) we find that the ligand NH_2 group can interact (in the NH_3^+ form) with D87 in IspG, similar to the proposed E126/NH_3^+ interaction for IspH (based on the X-ray structure of the rotated-out conformer), as illustrated in Figure 7A. To help test this hypothesis we used a D87A *Thermus thermophilus* IspG mutant. With this mutant there is essentially no EPR signal observed in the absence of any ligand, Figure S13A and only a very weak signal in the presence of **7**, Figure S13). However, in the presence of HMBPP (**2**) the spectrum (Figure S13C) is essentially the same as that seen with the other, wild-type proteins, suggesting that D87 is involved in binding of the amino-HMBPP (**7**), but not HMBPP itself. With HMBPP and the thiol ligand **8**, we therefore propose that both bind as weak π-complexes to the 4th Fe, as illustrated for **2** in Figure 7B.

Binding of acetylene inhibitors to IspG

Finally, we investigated the EPR and ENDOR spectra of the two specifically ^{13}C-labeled acetylene inhibitors, **5**. We show the EPR spectra of **5** bound to *Ec*IspG in Figure 8A, B, as well as the Davies ENDOR spectra of [3-^{13}C]-**5** and [4-^{13}C]-**5** bound to *Ec*IspG, in Figure 8C, D. The *g*-values found (by spectral simulation) for **5** bound to *Ec*IspG are 2.087, 2.012 and 2.003, leading to g_{iso} = 2.034 and Δg = 0.085, Table S1 and Figure 3. These values are similar to those found with the reactive intermediate "X" bound to both *Ec*IspG as well as *T. thermophilus* IspG, shown in Table S1 (g_1 ~2.09, g_2 ~2.02; g_3 = 2.00; g_{iso} = 2.04; Δg ~0.09) and Figure 3. In previous work[22] we proposed that "X" arose from a $[Fe_4S_4]^{3+}$ $S = {}^1/_2$ HiPIP-like cluster and, based on these *g*-values, extensive charge transfer to the acetylene **5** due to metal-alkyne π interactions seems likely. We also find sizeable ^{13}C hyperfine couplings, and from field dependence and spectral simulation results (Figure 8, green) we determined the principal components of the two hyperfine tensors. For [4-^{13}C]-**5** (i.e. labeled at the terminal carbon), we obtain $\boldsymbol{A_{ii}}$ = [5.4 1.5 3.8] MHz, and for [3-^{13}C]-**5**, we find $\boldsymbol{A_{ii}}$ = [4.5 3.0 10] MHz, Figure 8C, D. These tensors indicate close proximity of the acetylene group to the reduced 4Fe-4S cluster, facilitating, we propose, a strong pi interaction. To obtain estimates of the distances involved, we employed the point dipole approximation.[29] Using the largest diagonal component of the anisotropic hyperfine tensor together with previously reported spin-projection coefficients for aconitase[29] leads to Fe-C_3 distances in the range 2.0–2.6 Å, and Fe-C_4 distances in the range 2.6–3.2 Å. Since the sum of the Fe and C van der Waals radii is ~ 3.5 Å,[30] these distances are indicative of Fe-C bonding. For HMBPP, the Fe-C2 and Fe-C3 distances are in the range ~2.3–2.9 Å, Table S3, again consistent with a weak pi interaction.

Conclusions

In summary: the results we have presented here are of interest for several reasons. First, we find that in addition to inhibiting IspH, both the amine (**7**) and thiol (**8**) ligands inhibit IspG, with IC_{50} values in the 0.8–2.5 μM range. Second, we find that the EPR spectra of **7** bound to IspH as well as **2** or **8** bound to IspG are indicative of π-bonding, with the amino/hydroxyl/thiol groups not directly bonded to Fe. The absence of a large ^{14}N hyperfine coupling for **7** bound to reduced IspH as well as the absence of a large ^{17}O hyperfine coupling for [1-^{17}O]-**2** bound to reduced IspG are consistent with these bonding proposals. Third, we find that the *g*-values for the acetylene inhibitor **5** bound to IspG suggest a π-interaction between Fe and the alkyne group,[33,34] and the ^{13}C hyperfine tensors for both carbons in the acetylene group of **5** in the complex with IspG also indicate Fe-C bonding. Fourth, the binding of **7** to IspG (see Figure S12) as well as of **8** to IspH did not result in any π-interaction type EPR spectra, and with **8** it appears that the 4Fe-4S cluster in IspH is not reduced by dithionite. These results show, then, an unexpected diversity in spectroscopic behavior – and hence binding modes – for three IspG/IspH inhibitors, results that are of interest in the context of anti-infective drug design targeting isoprenoid biosynthesis. In particular, the possibility of developing leads that inhibit both IspG as well as IspH is likely to be of importance in decreasing resistance, as well as reducing the pro-inflammatory effects of **2** in acute infections[35] that would be expected to occur with solely IspH inhibition.

Experimental

Chemical Synthesis

The NH_2- (**7**) and SH- (**8**) analogs of HMBPP, as well as [1-^{13}C], [2-^{13}C], and [3-^{13}C]-HMBPP, were from the batches described previously.[31,32] In addition, in order to investigate bonding of the acetylene **5**, we synthesized both [3-^{13}C]-**5** and [4-^{13}C]-**5**, as described in the Supporting Information, in order to unambiguously determine the hyperfine coupling tensor elements, $\boldsymbol{A}_{ii}$, for each site.

CW-EPR/ENDOR/HYSCORE spectroscopy

All CW (continuous wave)-EPR experiments were performed on a Varian E-line 122 X-band spectrometer with an Air Products helium cryostat. Typical data acquisition parameters were: microwave frequency = 9.05 GHz; field center = 3250 G; field sweep = 1000 G; modulation frequency = 100 kHz; modulation amplitude = 5 Gauss; time constant = 32 ms; temperature = 8 – 20 K.

Pulsed ENDOR/HYSCORE spectra were obtained on a Bruker ElexSys E-580-10 FT-EPR EPR spectrometer equipped with an Oxford Instruments CF935 cryostat. A Bruker RF amplifier (150 watts, 100 kHz -250 MHz) was used for ENDOR experiments. Davies ENDOR used a three-pulse sequence $\pi_{mw} - t - \pi/2_{mw} - \tau - \pi_{mw} - \tau -$ echo; $\pi/2_{mw}$ = 96 ns, with π_{RF} (10 μs, 3 dB attenuation) applied during *t*. HYSCORE used a four-pulse sequence $\pi/2_{mw} - \tau - \pi/2_{mw} - t_1 - \pi_{mw} - t_2 - \pi/2_{mw} -$ echo; $\pi/2_{mw}$ = 16 ns and π_{mw} = 32 ns, 128 points for both t_1 and t_2, each using 24 ns steps. Time-domain data were baseline corrected using a 3rd order polynomial, and then Hamming windowed, followed by zero-filling, and 2D-Fourier transformation and symmetrization. Parameters were typically: microwave frequency = 9.65 – 9.72 GHz, temperature = 8 – 15 K, microwave power attenuation = 6.5 – 9 dB.

Supplementary Material

Refer to Web version on PubMed Central for supplementary material.

Acknowledgments

This work was supported by NIH Grant GM065307 (to E. O.). W.W. and J.L. were both supported by predoctoral fellowships from the American Heart Association, Midwest Affiliate (awards 10PRE4430022 to W.W. and 11PRE7500042 to J.L.). We would like to thank Dennis Dean for providing the *isc* protein expression system, Pinghua Liu for providing the *E. coli* IspG expression system, Manuel Rodriguez-Concepción for providing the *A. thaliana* IspG expression system, Hassan Jomaa and Jochen Wiesner for providing the *A. aeolicus* IspH, *P. falciparum* IspH, and *T. thermophilus* IspG expression systems, and Mark J. Nilges for assistance with the EPR spectroscopy.

Notes and references

1. Zhao L, Chang W, Xiao Y, Liu H, Liu P. Annu Rev Biochem. 2013; 82:497–530. [PubMed: 23746261]
2. Gräwert T, Groll M, Rohdich F, Bacher A, Eisenreich W. Cell Mol Life Sci. 2011; 68:3797–3814. [PubMed: 21744068]

3. Heuston S, Begley M, Gahan CGM, Hill C. Microbiology. 2012; 158:1389–1401. [PubMed: 22466083]
4. Rekittke I, Wiesner J, Röhrich R, Demmer U, Warkentin E, Xu W, Troschke K, Hintz M, No JH, Duin EC, Oldfield E, Jomaa H, Ermler U. J Am Chem Soc. 2008; 130:17206–17207. [PubMed: 19035630]
5. Gräwert T, Span I, Eisenreich W, Rohdich F, Eppinger J, Bacher A, Groll M. Proc Natl Acad Sci. 2010; 107:1077–1081. [PubMed: 20080550]
6. Rekittke I, Nonaka T, Wiesner J, Demmer U, Warkentin E, Jomaa H, Ermler U. FEBS Lett. 2011; 585:447–451. [PubMed: 21167158]
7. Lee M, Gräwert T, Quitterer F, Rohdich F, Eppinger J, Eisenreich W, Bacher A, Groll M. J Mol Biol. 2010; 404:600–610. [PubMed: 20932974]
8. Rekittke I, Jomaa H, Ermler U. FEBS Lett. 2012; 586:3452–3457. [PubMed: 22967895]
9. Liu YL, Guerra F, Wang K, Wang W, Li J, Huang C, Zhu W, Houlihan K, Li Z, Zhang Y, Nair SK, Oldfield E. Proc Natl Acad Sci. 2012; 109:8558–8563. [PubMed: 22586085]
10. Wang W, Wang K, Liu YL, No JH, Li J, Nilges MJ, Oldfield E. Proc Natl Acad Sci. 2010; 107:4522–4527. [PubMed: 20173096]
11. Wang K, Wang W, No JH, Zhang Y, Zhang Y, Oldfield E. J Am Chem Soc. 2010; 132:6719–6727. [PubMed: 20426416]
12. Wang W, Li J, Wang K, Smirnova TI, Oldfield E. J Am Chem Soc. 2011; 133:6525–6528. [PubMed: 21486034]
13. Wang W, Li J, Wang K, Huang C, Zhang Y, Oldfield E. Proc Natl Acad Sci. 2010; 107:11189–11193. [PubMed: 20534554]
14. Ahrens-Botzong A, Janthawornpong K, Wolny JA, Tambou EN, Rohmer M, Krasutsky S, Poulter CD, Schünemann V, Seemann M. Angew Chem Int Ed. 2011; 50:11976–11979.
15. Scott, RA.; Lukehart, CM. Applications of Physical Methods to Inorganic and Bioinorganic Chemistry. John Wiley & Sons; 2007.
16. Schweiger, A.; Jeschke, G. Principles of Pulse Electron Paramagnetic Resonance. Oxford University Press; 2001.
17. Höfer P, Grupp A, Nebenführ H, Mehring M. Chem Phys Lett. 1986; 132:279–282.
18. Davies ER. Phys Lett A. 1974; 47:1–2.
19. Xu W, Lees NS, Hall D, Welideniya D, Hoffman BM, Duin EC. Biochemistry (Mosc). 2012; 51:4835–4849.
20. Beinert H, Kennedy MC, Stout CD. Chem Rev. 1996; 96:2335–2374. [PubMed: 11848830]
21. Span I, Gräwert T, Bacher A, Eisenreich W, Groll M. J Mol Biol. 2012; 416:1–9. [PubMed: 22137895]
22. Wang W, Wang K, Span I, Jauch J, Bacher A, Groll M, Oldfield E. J Am Chem Soc. 2012; 134:11225–11234. [PubMed: 22687151]
23. Jakobsen HJ, Hove AR, Hazell RG, Bildsøe H, Skibsted J. Magn Reson Chem. 2006; 44:348–356. [PubMed: 16477689]
24. Malkin R, Bearden AJ. Proc Natl Acad Sci. 1971; 68:16–19. [PubMed: 4322259]
25. Wang W, Wang K, Li J, Nellutla S, Smirnova TI, Oldfield E. J Am Chem Soc. 2011; 133:8400–8403. [PubMed: 21574560]
26. Stoll S, Schweiger A. J Magn Reson. 2006; 178:42–55. [PubMed: 16188474]
27. Stoll S, Britt RD. Phys Chem Chem Phys. 2009; 11:6614–6625. [PubMed: 19639136]
28. Trott O, Olson AJ. J Comput Chem. 2010; 31:455–461. [PubMed: 19499576]
29. Walsby CJ, Hong W, Broderick WE, Cheek J, Ortillo D, Broderick JB, Hoffman BM. J Am Chem Soc. 2002; 124:3143–3151. [PubMed: 11902903]
30. Batsanov SS. Inorg Mater. 2001; 37:871–885.
31. Span I, Wang K, Wang W, Jauch J, Eisenreich W, Bacher A, Oldfield E, Groll M. Angew Chem Int Ed. 2013; 52:2118–2121.
32. Li J, Wang K, Smirnova TI, Khade RL, Zhang Y, Oldfield E. Angew Chem Int Ed. 2013; 52:6522–6525.

33. Lee H-I, Igarashi RY, Laryukhin M, Doan PE, Dos Santos PC, Dean DR, Seefeldt LC, Hoffman BM. J Am Chem Soc. 2004; 126:9563–9569. [PubMed: 15291559]

34. Ryle MJ, Lee HI, Seefeldt LC, Hoffman BM. Biochemistry (Mosc). 2000; 39:1114–1119.

35. Davey MS, Lin CY, Roberts GW, Heuston S, Brown AC, Chess JA, Toleman MA, Gahan CGM, Hill C, Parish T, Williams JD, Davies SJ, Johnson DW, Topley N, Moser B, Eberl M. PLoS Pathog. 2011; 7:e1002040. [PubMed: 21589907]

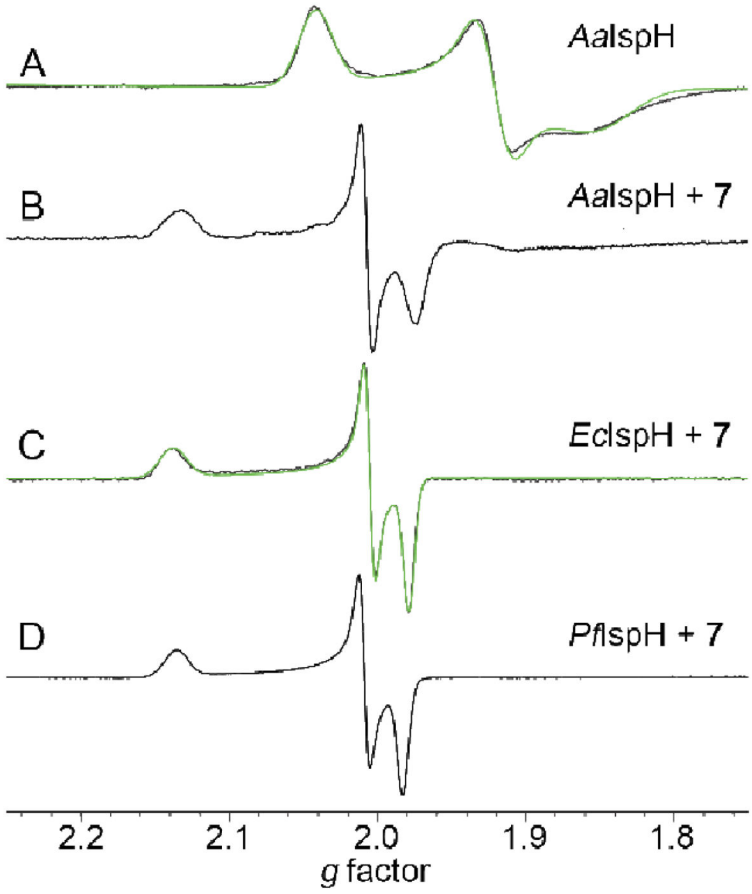

Figure 1.

9.05 GHz CW-EPR spectra of IspHs. (A) 1.3 mM *Aa*IspH (reduced) + 20 eq dithionite. (B) 1 mM *Aa*IspH + 40 eq dithionite + 28 eq **7**. (C) 1.1 mM *Ec*IspH + 10 eq **7** + 30 eq DT. (D) 0.5 mM *Pf*IspH + 20 eq **7** + 80 eq DT. Spectra acquired at 10–24 K.

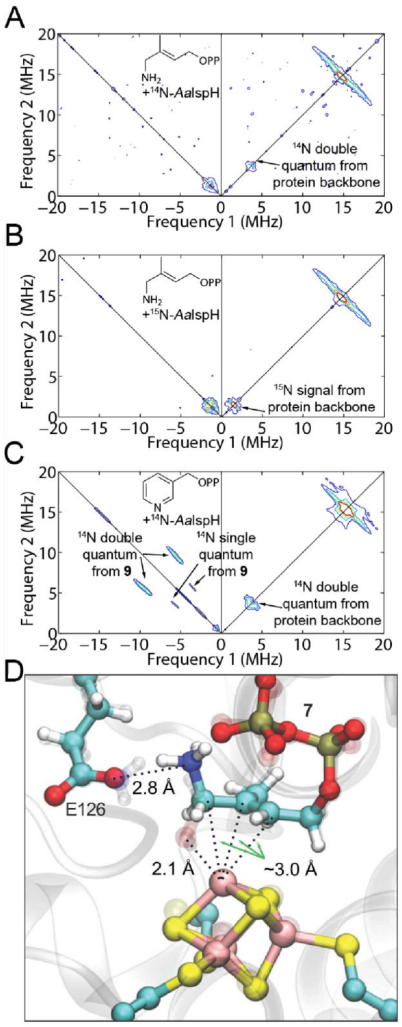

Figure 2.

HYSCORE spectra of IspH with nitrogen-containing inhibitors, and a model for the *Aa*IspH + **7** complex. (A) *Aa*IspH + **7**. T = 15 K, ν = 9.706 GHz, magnetic field = 3455 G, sum spectrum of τ = 136, 168, 200 and 256 ns. (B) ^{15}N-labeled *Aa*IspH + **7**. T = 15 K, ν = 9.712 GHz, magnetic field = 3460 G, sum spectrum of τ = 136, 168, 200 and 256 ns. (C) *Aa*IspH + **9** (adapted from Wang et al.[12]). T = 8 K, ν = 9.66 GHz, magnetic field = 3600 G, τ = 136 ns. (D) Model for binding of **7** (protonated, ammonium form) based on the X-ray structure of IspH + **2** (PDB ID 3KE8 and 3SZU, Span et al.[21])

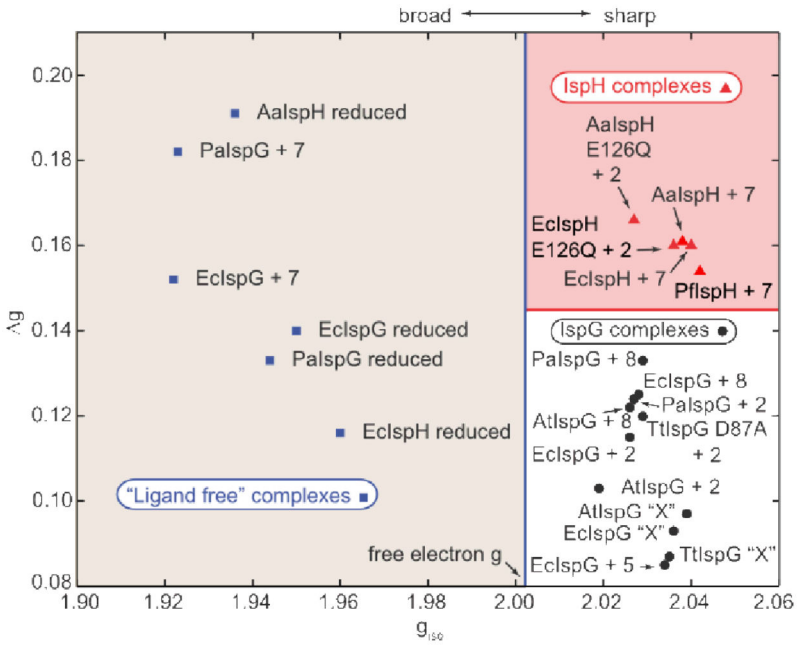

Figure 3.

Plot of Δg versus g_{iso} for IspH and IspG. Points to the left are proposed to originate from proteins in the absence of exogenous ligands bound to the cluster and are all broad; points on the right are all from sharp spectra and are proposed to originate from π/σ or HiPIP-like complexes.

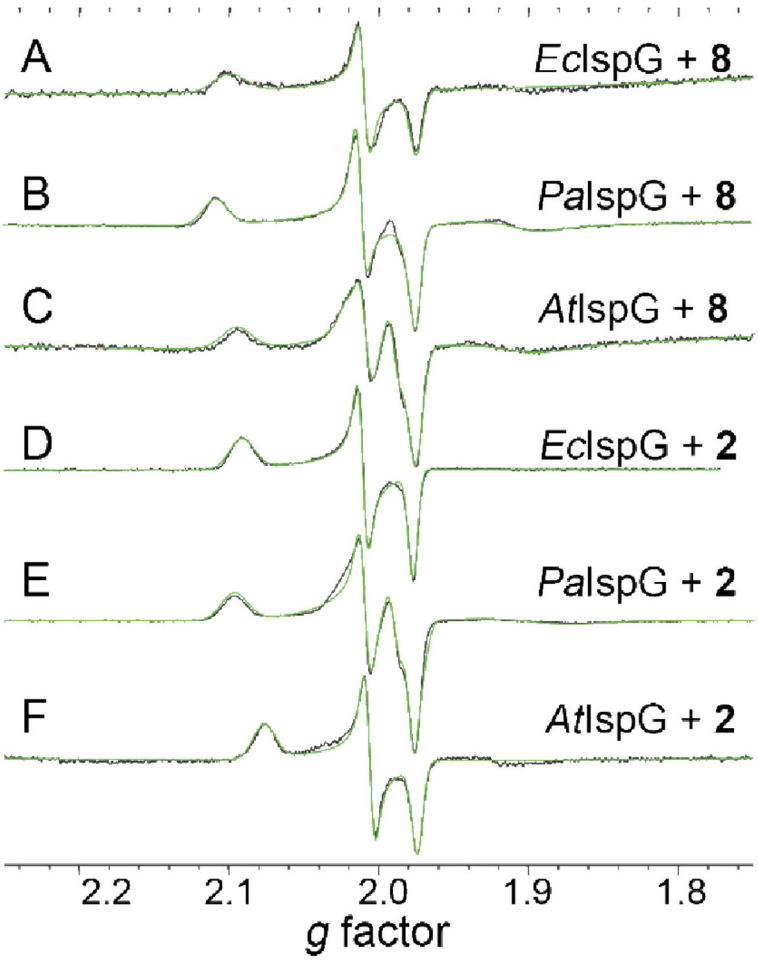

Figure 4.

9.05 GHz CW-EPR spectra (black) and spectral simulations (green) of *E. coli* (A, D), *P. aeruginosa* (B, E), and *Arabidopsis thaliana* (C, F) IspG in the presence of **8** (A–C) or **2** (D–F). *T* = 8K, Power = 5 mW. 500–600 μM IspG + 80 eq dithionite + 20–40 eq **8** or **2**.

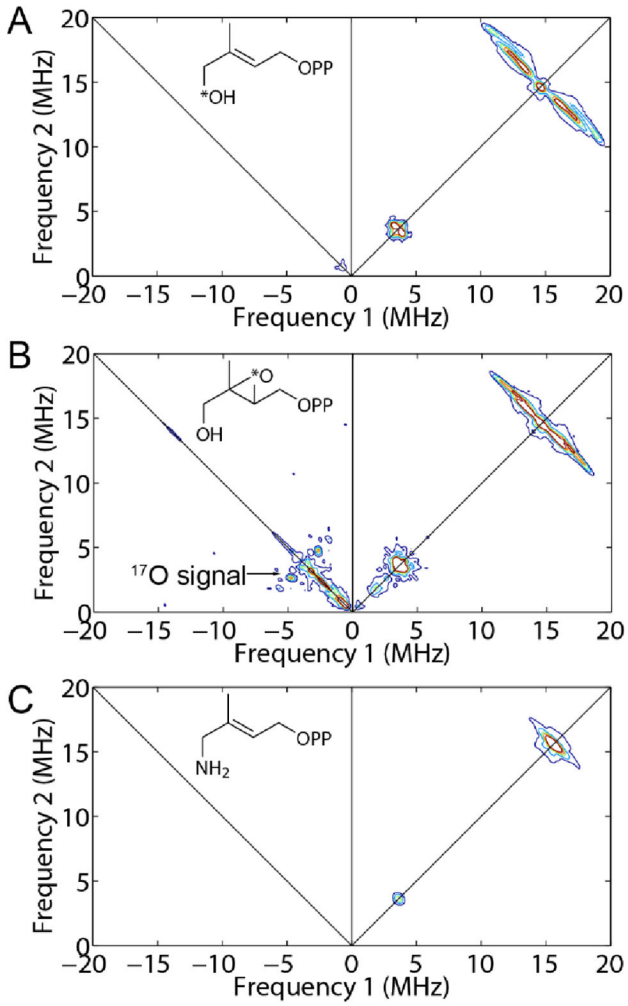

Figure 5.

9.66 GHz HYSCORE spectra of (A) [1-^{17}O]-2 (HMBPP) bound to *Pa*IspG. T = 10 K, magnetic field = 3435 G, τ = 136 ns. (B) HYSCORE of [2,3-^{17}O]-2 epoxide bound (as the ferraoxetane "X") to *Tt*IspG (adapted from Wang et al.[10]). T = 18 K, magnetic field = 3420 G, τ = 136 ns. (C) HYSCORE of 7 bound to *Pa*IspG. T = 8 K, magnetic field = 3660 G, τ = 136 ns.

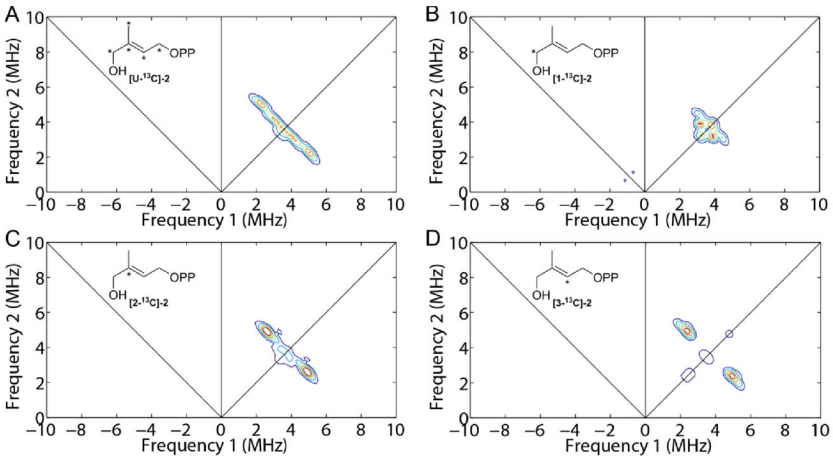

Figure 6.

9.7 GHz HYSCORE spectra of ^{13}C labeled **2** bound to PaIspG. (A) [*U*-^{13}C]-**2** + *Pa*IspG. Magnetic field = 3315 G, τ = 136 ns. (B) [1-^{13}C]-**2** + *Pa*IspG. Magnetic field = 3480 G, τ = 136 ns. (C) [2-^{13}C]-**2** + *Pa*IspG. Magnetic field = 3435 G, τ = 136 ns. (D) [3-^{13}C]-**2** + *Pa*IspG. Magnetic field = 3315 G, τ = 136 ns. 1-1.7 mM *Pa*IspG + 40 eq dithionite + 16–20 eq ^{13}C labeled **2**. *T* = 10 K.

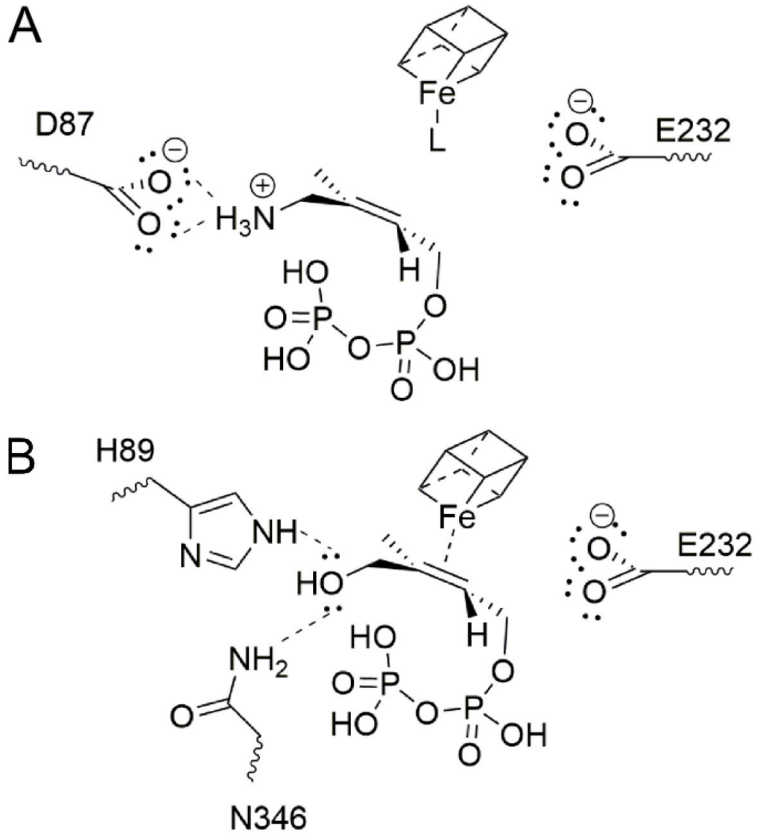

Figure 7.
Proposed binding of (A) **7** and (B) **2** to IspG (*T. thermophilus residue numbering*). The nature of L in (A) is unknown.

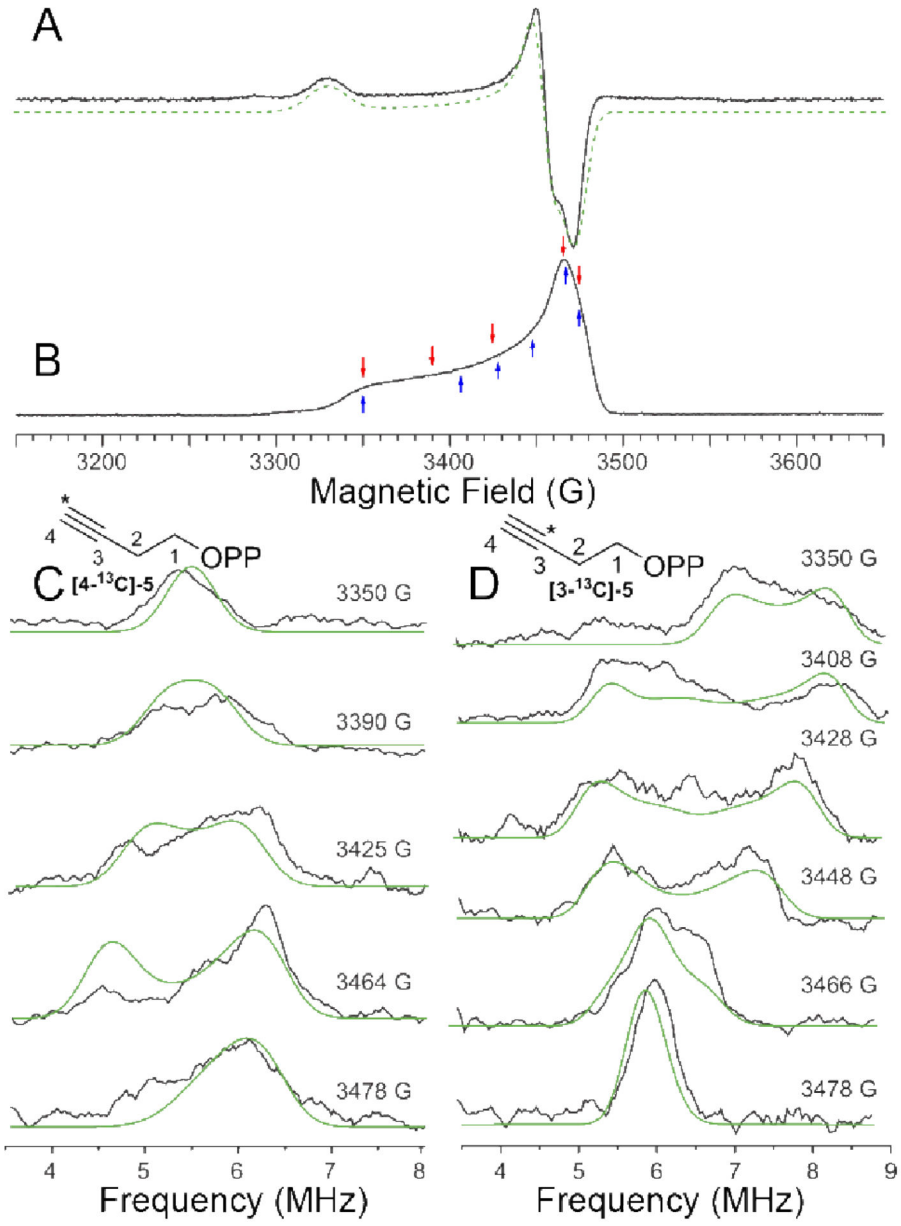

Figure 8.

9.7 GHz (A) CW-EPR and (B) swept-spin echo spectrum of *Ec*IspG + **5**, *T* = 15 K. Simulation of spectrum in (A) yields $\boldsymbol{g_i}$ = [2.003, 2.012, 2.087]. Microwave frequency = 9.729 GHz for (A) and 9.758 for (B). Arrows indicate the magnetic fields at which the ENDOR spectra in (C) and (D) were obtained. (C) 9.7 GHz ^{13}C Davies ENDOR spectra of *Ec*IspG + [4-^{13}C]-**5**. The principal components of the ^{13}C hyperfine coupling tensor are $\boldsymbol{A_{ii}}$ (4-^{13}C) = [5.4 1.5 3.8] MHz. Euler angles are α = 32°, β = γ = 0°. (D) 9.7 GHz ^{13}C Davies ENDOR of *Ec*IspG + [3-^{13}C]-5. $\boldsymbol{A_{ii}}$ (3-^{13}C) = [4.5 3.0 10] MHz and Euler angles are α = 80°, β = 30° and γ = 60°. Simulations are in green.

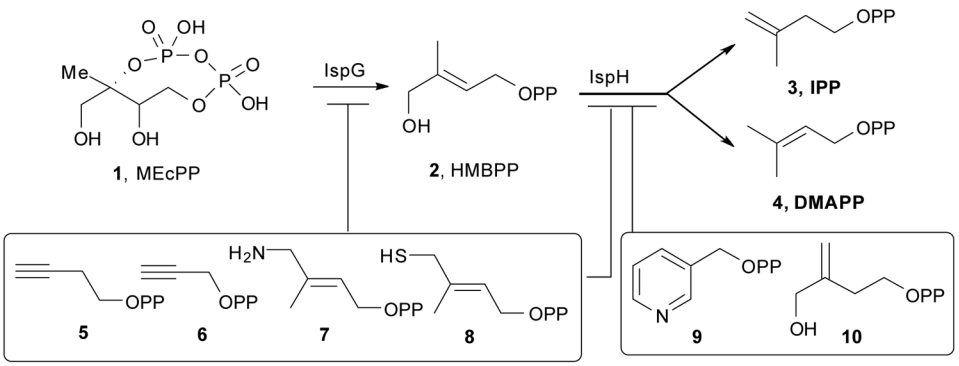

Scheme 1.
IspG- and IspH-catalyzed reactions and their inhibitors.